# Polymer Adhesion vs Substrate Receptor Group Density

**Ilsoon Lee and Richard P. Wool***

*Department of Chemical Engineering, University of Delaware, Newark, Delaware 19716*

*Received June 28, 1999; Revised Manuscript Received January 14, 2000*

ABSTRACT: The effect of substrate receptor group density on polymer adhesion was investigated. Model substrates with varying $-NH_2$ density on $Al_2O_3$ were prepared by a self-assembly of mixed amine-terminated silanes and methyl-terminated silanes. The model polymer was synthesized through a high-pressure carboxylation of polybutadiene. The polymer adhesion was determined by the fracture energy of the polymer−solid interfaces, $G_{IC}$, from a T-peel test. The strong acid−base interactions between the polymer sticker groups (−COOH) and the substrate receptor groups ($-NH_2$) at the interface caused an interesting fracture energy variation in the range of annealing times examined. At short time, $G_{IC}$ increased as the density of substrate receptor groups increased. However, at long time, $G_{IC}$ increased up to 30% receptor group coverage and then decreased with increasing coverage. A maximum in $G_{IC}$ occurred because the adhesive interface strength increased between the solid surface and the adsorbed chains, and simultaneously the cohesive interface strength decreased between the adsorbed chains and the neighboring free chains with increasing density. Failure occurred at the weaker of the two interface strengths. In this paper, it was shown that the polymer adhesion was not a monotonic function of the surface energetics.

## 1. Introduction

Polymer adhesion has been studied extensively for its important applications in industrial processes, such as composite manufacturing and durability, coatings, and packing for microelectronics components. Since the structure and strength of polymer−solid interfaces are closely related to each other, the fundamental understanding of the behavior of polymer chains near the solid surface is crucial in optimizing the interfacial strength in such systems.[1−3]

Generally polymers can be functionalized to enhance the adhesion of the polymer to the solid surfaces.[4−6] For example, the addition of carboxylic acid sticker groups abruptly enhances the adhesion of polybutadiene (PBD) to aluminum. The surface of solid substrates can also be functionalized to enhance the polymer adhesion. For these modifications, many industrial techniques are used. Plasma, laser treatments, corona, UV, ozone, and chemical modification treatments were developed for such purposes.[7,8] However, most research has been limited to determining the effect of the extent of modification on the improvement in material properties. The interplay of polymer sticker groups (−X) and substrate receptor groups (−Y) is the main factor controlling the strength of the polymer−solid interface. Here, we defined the problem as the X−Y problem at the polymer−solid interface, as shown in Figure 1. The interplay requires an interfacial chain restructuring process, which depends on the amount of X and Y.

In regard to the X problem of polymer adhesion, various copolymer−substrate systems have been studied. In 1949, Mclaren and Seiler[9] found that the maximum fracture energy was obtained, when 1.6% of maleic acid was added as a sticker group in the aluminum/vinyl chloride−vinyl acetate−maleic acid terpolymer system. They concluded that too much maleic acid groups caused excessive corrosion of the aluminum substrate. In 1962, Mao and Reegen[10] studied a similar system, epoxy ester resin/methyl methacrylate−acrylamide copolymers, to find that the adhesion energy showed optimum behavior as a function of the acrylamide, at about 10 mol %. They argued that the phenomenon was due to the increase of the crystallinity with further addition of acrylamide. Schultz et al.[11] also found the optimum behavior of the interfacial fracture energy of aluminum/maleic anhydride grafted polypropylene system. They explained that a weak boundary layer formed with low molecular weight grafted chains, which formed during the grafting reaction, decreasing the cohesive strength. Recently, a new explanation has come to explain this optimum behavior in polymer−solid adhesion. In 1998, Gong et al.[12] showed that a critical concentration of sticker groups gave the optimal chain connectivity near the surface that caused the maximum fracture energy, as shown in Figure 2. They used a carboxylated polybutadiene (cPBD)−$Al_2O_3$ substrate system to show that the cohesive strength, $G_{IC}$, of the copolymer increased with increasing sticker groups up to a maximum, after which $G_{IC}$ decreased due to the dense attachment of sticker groups to the solid surface. Gutman and Chakraborty[13] have also argued that the optimum behavior of the fracture energy might originate from chain orientation and conformation within the interfaces. In the same way, Beck Tan et al.[14] studied the interfaces of a sulfonated polystyrene−poly(2-vinylpyridine) system. The interfacial fracture energy increased with up to 5−7 mol % sulfonation reaction and then decreased with further reaction at the inter-

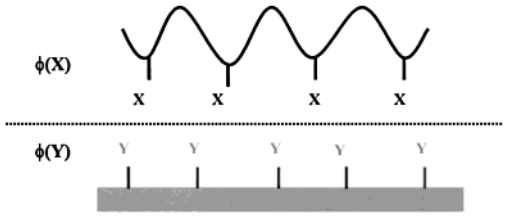


**Figure 1.** Schematic representation of the X−Y problem at a polymer−solid interface. X represents specific polymer sticker groups, and Y represents specific substrate receptor groups. $\phi$ is the mole percent or the mole fraction of the groups.

* To whom all correspondence should be addressed. E-mail wool@ccm.udel.edu.

10.1021/ma991037a CCC: $19.00 
Published on Web 03/08/2000

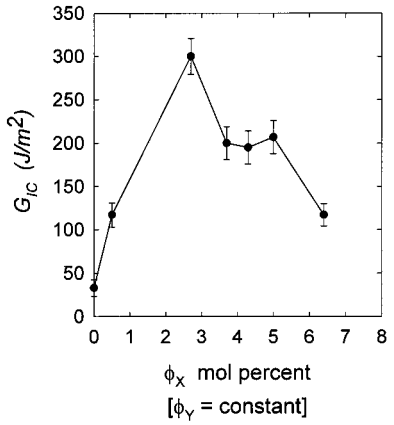


**Figure 2.** Sticker group (X) effect on the fracture energy of a cPBD−$Al_2O_3$ interface by Gong et al.[12] Here $\phi$(Y) is constant and X is COOH.

face. They explained that the decreasing fracture energy was due to the excessive interfacial bonding density at the interfaces, which caused the interfacial chains to entangle with themselves rather than with the chains in the bulk.

On the other hand, few studies have been done on the Y problem of polymer adhesion. The substrate active receptor group concentration, $\phi$(Y), is important, because the strong polymer−solid interface is made by the interactions of the polymer sticker groups, X, with the substrate receptor groups, Y. In this regard, the optimum value of $\phi$(X) should depend on $\phi$(Y). In addition, $\phi$(Y) strongly affects the restructuring process of an interfacial polymer chain, which determines the adhesion kinetics. Typically, most polymer adhesion studies have been discussed after short annealing times. The restructuring process of a chain near an interface could be quite longer than the relaxation time of a free bulk chain. New models have been proposed that predict the polymer adhesion from Y type and its coverage. However, their models have failed to explain our results. Generally, different methods of substrate surface treatment have been compared to the surface energetics relating to thermodynamic work of adhesion, which can be useful but misleading. In 1978, Fowkes and Mostafa[15] related the work of adhesion to the enthalpy of acid−base interaction. Their relation predicted that the work of adhesion increases with increasing number of acid−base pairs per unit area of interface. In 1981, Donnet[16] demonstrated the effects of the surface treatment of Al on the surface energy and work of adhesion in NBR (butadiene−acrylonitrile) and SBR (styrene−butadiene) elastomers. The measured adhesive strength was different from the calculated value from the surface tension. The mode of failure was cohesive for phosphatised and anodized Al but interfacial or adhesive for anodized sealed Al. They concluded that the thermodynamic work of adhesion calculated by the surface tension of the Al surfaces was not useful for predicting the order of real adhesive strengths of those systems, because the mode of failure was not interfacial in each case. Recently, Harding and Berg[17] studied the polymer adhesion in a filled poly(butyral) composite by varying a diaminosilane monolayer coverage on the filler particles after a relatively short annealing time. They found that the fracture strength increased with increasing coverage but did not increase further with multilayer coverage.

**Scheme 1. A Scheme of the Model Polymer Synthesis: Carboxylated Polybutadiene**

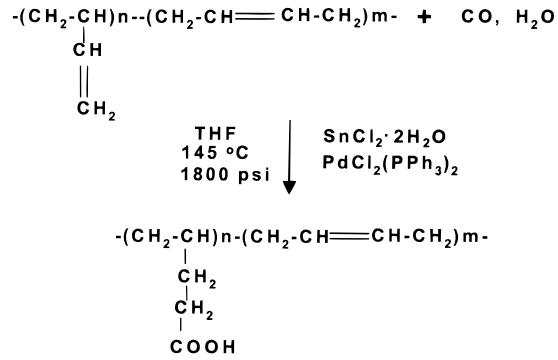


The objective of this work is the fundamental understanding of the Y effect on the polymer adhesion with well-defined model polymer−substrate systems. Several studies on the X problem of polymer adhesion have suggested that an optimum amount of the polymer sticker groups could be designed in the polymer adhesion problem. However, few fundamental studies have been done on Y problem of polymer−solid adhesion.

## 2. Experimental Section

**2.1. Carboxylated Polybutadiene (cPBD) Synthesis.** Polybutadiene (PBD) was chemically modified to have a certain amount of carboxylic acid sticker groups, $\phi_X$(COOH), using a high-pressure carboxylation reaction, as shown in Scheme 1. The procedures are briefly summarized below, and further details can be found elsewhere.[12,18] Polybutadiene (Firestone Diene 35A) with $M_n$ = 98 000, $M_w$ = 180 000, and 10 mol % vinyl (1,2 addition) groups was supplied by Firestone Rubber & Latex Co. A 100 mL THF solution consisting of PBD (2.04 g), $PdCl_2(PPh_3)_2$ (0.280 g), $SnCl_2{\cdot}2H_2O$ (0.902 g), and $H_2O$ (3.6 mL) was prepared and transferred to a Parr mini-300 stainless steel reactor. All the catalysts described above were purchased from Aldrich. The reactor containing the solution was pressurized at room temperature to 500 psi with CO and then released. This was done three times. After that, the reactor was pressurized again at room temperature to 1350 psi. An electric coil heater with a control unit was used to increase the reaction temperature to 145 °C and the pressure to around 1800 psi. A magnetic stirrer was used to facilitate the exchange of the surface exposed to the CO gas. The reaction time was 20 h. Finely dispersed solution containing palladium black, revealed upon the discharge of the reactor, was removed by centrifugation at 4000 rpm for 90 min. The polymer products were recovered from the solution by precipitation from a 100 mL mixture of solvent containing methanol (80 mL) and acetone (20 mL) and several drops of concentrated hydrochloric acid.

**2.2. Characterization of Polymer Sticker Groups.** The extent of carboxylation of cPBD, $\phi_X$(COOH), was determined via FTIR. A KBr liquid cell was used for the quantification of $\phi_X$(COOH) of cPBD in THF solution. A standard calibration curve was prepared using dicarboxy-terminated polybutadiene (dPBD), $M_n$ = 4200, which was purchased from Aldrich. $\phi_X$(COOH) of cPBD was quantified by comparing the net absorbance of the carbonyl groups (~1730 cm$^{-1}$) to the calibration curve constructed with dPBD. Spectra were obtained on a Mattson Genesis Fourier transform infrared spectrometer using 4 cm$^{-1}$ resolution and 64 scans. It was determined that approximately 120 of 4000 PBD monomer units have −COOH sticker groups. cPBD was a rubberlike material with a very low glass transition temperature, $T_g$, of −88 °C, which was determined by DSC measurement. Other characterization results of cPBD can be found elsewhere.[12,18]

**2.3. Preparation of Model Substrates (AlS).** The model substrates with varying density of amine base receptor groups $\phi_Y(NH_2)$ on $Al_2O_3$ were prepared using a self-assembly of mixed

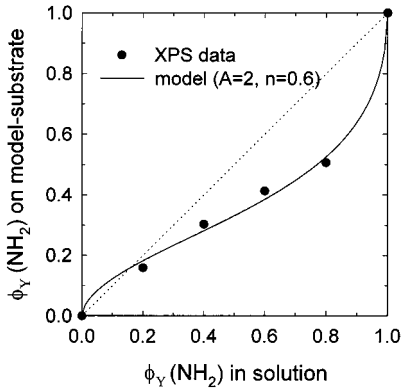


**Figure 3.** Solution composition vs surface composition: AS mole fraction on $Al_2O_3$.

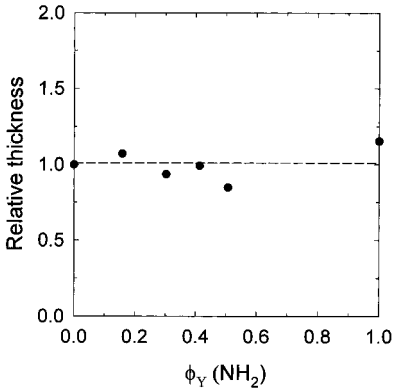


**Figure 4.** Relative thickness of the mixed monolayer-like silane coatings.

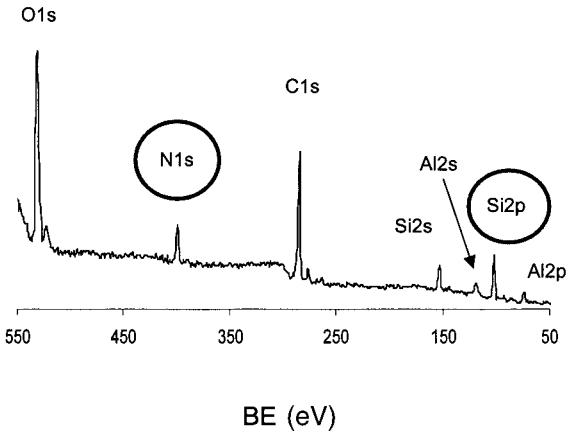


**Figure 5.** XPS spectrum of AS multilayers on $Al_2O_3$.

amine-terminated silanes (AS = $\gamma$-aminopropyltrimethoxysilane; $H_2NCH_2CH_2CH_2Si(OMe)_3$) and methyl-terminated silanes (MS; *n*-propyltrimethoxysilane; $CH_3CH_2CH_2Si(OMe)_3$) purchased from United Chemical Technologies Inc. As seen above, the structural difference between the two silanes was that AS had a primary amine group where MS did not have an amine group at the terminal carbon chain. Thus, MS was used to decrease the substrate active receptor groups $\phi_Y(NH_2)$ via competitive adsorption reaction from the mixed silane−water solutions to $Al_2O_3$. The methoxy groups (−OMe) of the silanes were hydrolyzed to form silanol-containing species ($-Si(OH)_3$). The silanol-containing species were highly reactive intermediates, which were responsible for bond formation with the substrate functional groups (Al−OH). The general mechanism for silane bond formation can be found elsewhere.[19,20]

The Al foil, purchased from Shim Stock Inc., was first pretreated overnight at 300 °C in an oven to ensure the formation of a stable layer of native oxide. The thickness of the Al foil was 25 $\mu$m, and the roughness average (RA) was determined to be about 0.5 $\mu$m using a scanning white light interferometer (SWLI). The kinetics and the packing of silane depositions were known to depend on concentration, reaction time, temperature, and pH of the solution.[20] In this work, the reaction time, temperature, and pH were kept constant. Varying the concentration of AS and MS changed the $-NH_2$ density on the model substrates. The total combined concentrations of AS and MS were 50 mM (ca. 0.8 wt %) in the mixed silane−water solutions. Figure 3 shows the mole fraction of AS in the mixed silane solutions and the result of the determination of densities on $Al_2O_3$, which will be explained in next section. The mixed AS and MS were placed on the Al oxide by dipping the Al substrates into the freshly prepared mixed silane water solutions at room temperature. The dipping time was 5 min, and the pH of the solutions was set to approximately 4.5 using several drops of acetic acid. Then, the silane-treated substrates were rinsed with copious amounts of distilled water to prepare monolayer-like silane coatings, then dried at room temperature, and finally cured in an oven under $N_2$ purging at 115 °C for 30 min. Generally, no rinsing made several layers of silanes on $Al_2O_3$, which might not be uniform in thickness as a function of AS mole fraction. During the hydrolysis and condensation reactions followed by the silane deposition, the first layer was strongly anchored to $Al_2O_3$ by the surface reaction of the silanol-containing species with the surface functional groups (Al−OH). However, the other layers were physically and weakly deposited on the first layer before rinsing procedure. The weakly deposited layers were not appropriate for this study, since they might complicate the failure mode of the interface. After the rinsing procedure only tightly anchored layers were believed to remain on $Al_2O_3$. The careful rinsing procedure has been performed to develop so-called "self-assembled monolayers" (SAMs). In this work, however, it was not clear whether the model substrates were monolayers, so they will be called "monolayer-like silane coatings" in this paper.

**2.4. Characterization of Model Substrates.** A Leybold-Heraeus XPS was used for the surface composition analysis of the model-substrates. This system has a monochromatic Mg K$\alpha$ X-ray source ($h\nu$ = 1253.6 eV). The XPS spectrum gave an average composition of the entire silane layers, more or less weighted to the surface, since Al peaks were also observed. It was assumed that most of the available Al−OH groups on $Al_2O_3$ were taken by either AS or MS. To confirm the uniform thickness or uniform coverage of the monolayer-like silane coatings, the relative Si peak intensities at various $\phi_Y$ were compared using eq 1

$$\text{Relative Thickness or Coverage} = \frac{I(\text{Si 2p})}{I(\text{Si 2p})|_{(\text{MS})}} \qquad (1)$$

where $I$ is the peak intensity of the atomic component on the coated substrates. Figure 4 shows that the relative Si peak intensities were approximately constant as $\phi_Y$ was varied. The sampling depth of XPS is 40−100 Å, and the length of an AS molecule is about 8 Å. The monolayer-like silane coatings showing weak Si peaks and strong Al peaks were prepared and used in the entire work. However, the silane multilayers showing strong N and Si peaks and weak Al peaks, as shown in Figure 5, which were prepared without the rinsing procedure, were used in the determination of the surface composition. The random distribution of AS was assumed in the silane mutilayers. The overlayer and the buried overlayer models, which will be discussed later, were not assumed to represent the AS distribution. It was known that the degradation of the top surfaces at a molecular level had normally been observed during XPS scanning in an ultrahigh-vacuum chamber.[21] A very weak N 1s peak but relatively strong Si peak of the monolayer-like silane coating by the pure AS coating was detected, even though the atomic sensitivity of N 1s is greater than that of Si 2p peak. We suspect that the X-ray degraded the $-NH_2$ layer exposed to it, but it did not degrade much of

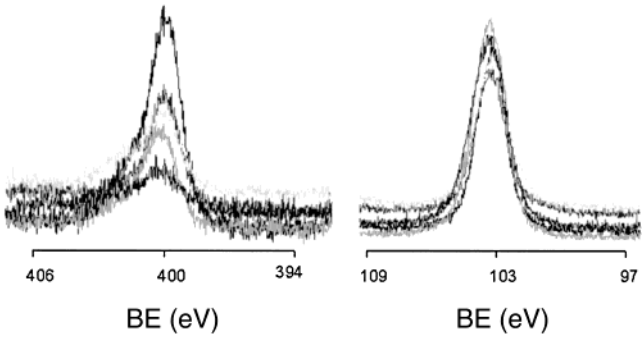


**Figure 6.** XPS peaks of N 1s (left) and Si 2p (right) of the mixed silane multilayers of AS and MS.

the anchoring atoms (Si) due to the greater depth of the Si. That is why we used the silane multilayers to determine the composition, which made it possible to detect every distinct peak, as shown in Figure 5. This would be fine as long as the random distribution of AS in the multilayers could be possibly assumed. The surface composition, mole fraction, was determined using eq 2 and the detailed XPS component scans as shown in Figure 6.

$$\phi_Y(NH_2) = \phi(AS) = \frac{\dfrac{I(\text{N 1s})}{I(\text{Si 2p})} - \left.\dfrac{I(\text{N 1s})}{I(\text{Si 2p})}\right|_{(MS)}}{\left.\dfrac{I(\text{N 1s})}{I(\text{Si 2p})}\right|_{(AS)} - \left.\dfrac{I(\text{N 1s})}{I(\text{Si 2p})}\right|_{(MS)}} \qquad (2)$$

Because of the different atomic sensitivities and the positions from the coating surface between N and Si atoms, the composition was normalized as shown in eq 2. For example, $\phi_Y$ of the pure AS treated substrates is 1, and that of a pure MS-treated substrate is 0. Hence, the composition of the mixed layers is between 0 and 1. It must be noted that carbon (C) was the main atomic component of impurities normally found on high energetic surfaces, and one AS molecule had one Si atom and one N atom, while one MS molecule had one Si atom but no N atom.

The competitive adsorption of AS and MS was analyzed using eq 3, which was derived using a kinetic model for the competitive adsorption of the mixed self-assembled monolayers (SAMs)[22,23] and fitted to determine the model parameters $A$ and $n$ of this system, as shown in Figure 3.

$$\phi_Y(NH_2)|_{\text{substrate}} = \phi(AS)|_{\text{substrate}} = \frac{1}{A\left.\left(\dfrac{\phi(MS)}{\phi(AS)}\right)^n\right|_{\text{solution}} + 1} \qquad (3)$$

where $A$ is the ratio of apparent surface reaction constant, $k'_{MS}/k'_{AS}$. Therefore, $A = 2$ roughly means that MS adsorbed to $Al_2O_3$ twice as fast as AS, and $n = 0.6$ means that the competitive adsorption reaction was negatively cooperative for AS.

An atomic force microscope (AFM) in TappingMode was used to see the silane coverage and two-dimensional distribution of AS and MS in the mixed monolayer-like silane coatings on $Al_2O_3$. The AFM images of $\phi_Y = 1$, $\phi_Y = 0$, and the pure $Al_2O_3$ were clearly different from each other. This was expected because the images were made from the contact force differences between the silicon tip of AFM and the model substrates. The AFM images of intermediate densities, between $\phi_Y = 1$ and $\phi_Y = 0$, appeared to be different from those of $\phi_Y = 1$, $\phi_Y = 0$, and the pure $Al_2O_3$; however, they were not clear enough to relate the images to the intermediate densities.

A CAHN dynamic contact angle analyzer using the Wilhelmy plate technique was used to investigate the wetting properties of the monolayer-like silane coatings on $Al_2O_3$. The

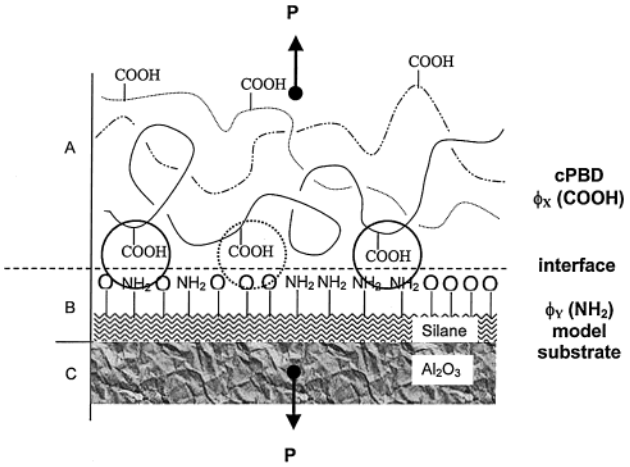


**Figure 7.** Schematic representation of the cPBD−AlS interface: (A) is the cPBD layer (16 $\mu$m), (B) is the mixed silane layer, and (C) is $Al_2O_3$. −O is the inert ($-CH_3$) functional groups. $\phi(NH_2) + \phi(CH_3) = 1$ on the model substrates. P is the load to peel.

water advance contact angle, $\theta_a(H_2O)$, of the surface with $\phi_Y = 1$ was measured to be 83.5° (±1.5°) and that with $\phi_Y = 0$ was 96.8° (±3°), 1 day after they were prepared and kept in a desiccator, while the contact angle for the untreated $Al_2O_3$ was 43°. The mixed monolayer-like silane coatings $0 < \phi_Y < 1$ showed large variations (6−11°) but gave $\theta_a$ values approximately along the linear interpolation line between the pure AS-treated and pure MS-coated substrates. A large variation of mixed monolayer-like silane layers was normally shown in other mixed self-assembled systems.[22,24] From the literature, the $\theta_a(H_2O)$ of monolayer-like silane coatings was reported as 88.4° (±4°)[25] for the AS-treated surface. $\theta_a(H_2O)$ of the monolayer-like silane coatings varied with the length and the packing of carbon backbone chains, as well as the terminal functional groups.[26] The $\theta_a(H_2O)$ was reported as 102° (±2°) for the *n*-butyltrichlorosilane-treated surface which has one more carbon chain (C4) relative to MS (C3), 62−76° for *tert*-butyltrchlorosilane (C4)-treated surfaces, and 112° (±2°) for octadecyltrichlrorosilane (C18)-treated surfaces.

It was believed that the distribution of AS and MS on $Al_2O_3$ was random. Evidence supporting this claim is as follows: The surface reaction is so fast that it can be considered random; the $Al_2O_3$ can be completely covered by silanes within a couple of minutes. Second, the surface anchoring groups of AS and MS are the same, and the molecular structures of AS and MS are similar to each other except for their terminal groups. In addition, contact angle measurements further confirmed that the surface is not an overlayer or buried overlayer, because the contact angle almost varied linearly between $\phi_Y = 1$ and $\phi_Y = 0$. Finally, AFM images showed that the mixed monolayer-like silane coatings did not look like one of $\phi_Y = 1$ and $\phi_Y = 0$.

**2.5. Interfacial Fracture Energy Determination.** The fracture energy, $G_{IC}$, of the cPBD−AlS interfaces, illustrated in Figure 7, was evaluated by a T-peel test. A layer of cPBD was uniformly cast onto the coated substrate from a 2 wt % solution of toluene. The thickness of the cPBD was estimated to be approximately 16 $\mu$m, based on the volume of solution cast, the surface area covered, and weight gain. After the toluene was evaporated under vacuum for 15 min, another coated substrate was then put on the top of the cPBD layer to form an AlS−cPBD−AlS sandwich structure. After being pressed together for 5 min to ensure good contact, the AlS−cPBD−AlS structure was annealed under 4 kPa pressure at room temperature for different times and then cut into specimens with dimensions of 60 mm in length and 10 mm in width. The peel tests were conducted on a Mini-44 Instron tensile machine at a crosshead speed of 30 mm/min. The fracture energy, $G_{IC}$, was obtained from the average of three

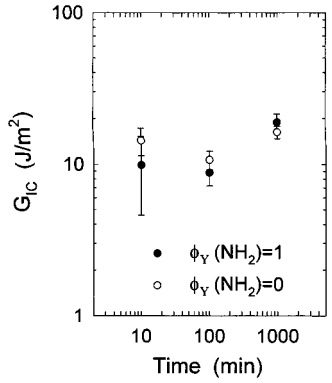


**Figure 8.** Fracture energy of the PBD−AlS interfaces.

tests per material and is given by

$$G_{IC} = \frac{2P}{b} \tag{4}$$

where $P$ is the peel load and $b$ is the width of the test sample.

## 3. Results and Discussion

**3.1. PBD/Model Substrate: Weak Interface.** As shown in Figure 8, the fracture energy, $G_{IC}$, of the pure PBD−AlS interfaces remained low, about 10 J/m$^2$, at all annealing times during our experiments. This was expected because $\phi_X(COOH) = 0$. The adhesive locus of failure was identified with the naked eye and an optical microscope. The pure PBD surface interacted with the model substrate by van der Waals forces. However, this $G_{IC}$ value of 10 J/m$^2$ was more than 2 orders of magnitude higher than the thermodynamic work of adhesion, $W_A \cong 0.10$ J/m$^2$, where only dispersive forces (van der Waals) existed.[27,28] The same value of $G_{IC}$ with $W_A$ was only expected for the thermodynamic reversible fracture. However, the fracture was an irreversible process. This will be discussed later with intrinsic interface strength. In Figure 8, no specific annealing time dependence on $G_{IC}$ was shown. This was expected because the reptation time, $T_r$, of PBD was only about 1.6 s at room temperature. The calculation of $T_r$ will be shown later. The difference in the substrates, $\phi_Y(NH_2) = 1$, $\phi_Y(CH_3) = 1$ ($\phi_Y = 0$), was not reflected on the value of $G_{IC}$ observed. In this paper $\phi_Y$ means $\phi_Y(NH_2)$, unless stated otherwise.

When the deformation rate, $R$, is greater than the inverse of the reptation time, $1/T_r$, the viscosity dominates the $G_{IC}$ of the polymer above the glass transition temperature. In this case, de Gennes suggested a crude approximation with $W_A$ using a viscoelastic trumpet analysis, where $G_{IC}$ was approximately given by[29]

$$G_{IC} = W_A R T_r \tag{5}$$

Substitution of all the values of $R$ (31.3 s$^{-1}$) and $T_r$ (1.6 s) gave a $G_{IC}$ value of 5 J/m$^2$. Here the deformation rate, $R$, was defined as the rate of peel divided by the film thickness. The fracture energy of polymer−solid interface was crudely estimated to be $RT_r$ times the thermodynamic work of adhesion, which was mainly the viscous dissipation contribution from the bulk polymers.

**3.2. cPBD/Model Substrate: Strong Interface.** When a few percent of sticker groups $\phi_X(COOH) = 2.9$ mol % was introduced onto the pure PBD, $G_{IC}$ showed remarkable changes with $\phi_Y(NH_2)$, as shown in Figure 9. It is interesting to note that $G_{IC}$ increased with

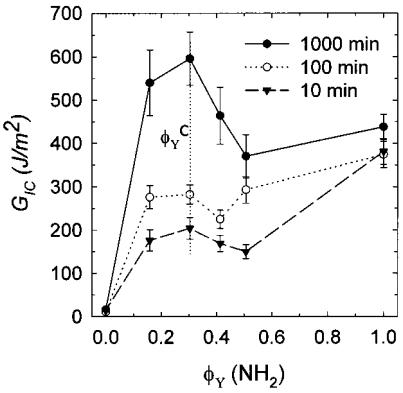


**Figure 9.** Fracture energy of the cPBD−AlS interfaces as a function of the substrate receptor group density, $\phi_Y(NH_2)$. On the model substrate, $\phi(NH_2) + \phi(CH_3) = 1$. The concentration of sticker group, $\phi_X(COOH)$, was about 3 mol %. The data point at $\phi_Y(NH_2) = 0$ is based on the pure dispersive forces of PBD.

increasing $\phi_Y$ up to the critical point $\phi_Y^c = 0.3$, and then it decreased with further increase in $\phi_Y$ for the long annealing time (1000 min). The other interesting result is that the long time dependence of $G_{IC}$ compared to the characteristic time of the polymer. This adhesion kinetics will be discussed in section 3.4.

Previously, an optimum sticker group concentration, $\phi_X^c$, was found in the fracture energy of the cPBD−$Al_2O_3$ interface as a function of carboxylic acid group concentration, $\phi_X(COOH)$,[12] which was shown in Figure 2. Beck tan et al.[14] also found such a behavior in the sulfonated polystyrene−poly(2-vinylpyridine) interface as a function of sulfonic acid group concentration, $\phi_X(SO_3H)$. Such an optimum $G_{IC}$ as a function of $\phi_X$ was explained by relating the sticker group concentration to the interfacial chain conformation. Gong and Wool[12] explained the result, shown in Figure 2, that the fracture energy of the polymer−solid interface is subject to the weaker of the adhesive strength and cohesive strength. When the amount of the sticker groups is small, increasing the sticker group concentration increases the adhesive strength. However, at high concentrations, the dense attachment of the near-surface layer to the solid substrate decreases the cohesive strength. Another possible explanation for these results is that the physical or chemical properties of the polymers could change more or less as a function of $\phi_X$, even though the molecular weight and its distribution on the polymer backbone chain remained the same during the addition of the sticker groups. Thus, it can be said that our results can confirm this explanation of the maximum failure energy behavior relating to the interfacial chain structure and connectivity. The details will be discussed further in this paper.

**3.3. Surface Energetics vs Fracture Energy.** The adhesion behavior of a polymer, shown in Figure 9, appears contrary to the popularly held concept that the fracture energy, $G_{IC}$, increases with the number of acid−base interactions, $n^{ab}$. For example, Fowkes and Mostafa[15] tried the quantitative analysis of the acid−base interactions. They related $W_A$ to the enthalpy of acid−base interaction $\Delta H^{ab}$ such that

$$W_A \sim \Delta H^{ab} n^{ab} \tag{6}$$

Thus, for our system, they would predict

$$G_{IC} \sim W_A \sim \phi_Y(NH_2) \tag{7}$$

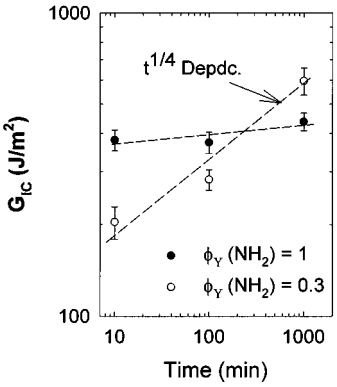


**Figure 10.** Adhesion kinetics of cPBD−AlS interfaces at low energetic surface ($\phi_Y = 0.3$) and at high energetic surface ($\phi_Y = 1$).

where both $G_{IC}$ and $W_A$ are expected to increase with increasing $\phi_Y(NH_2)$ at constant $\phi_X(COOH)$. However, $G_{IC}$ increased with increasing $\phi_Y$ until the critical point, $\phi_Y^c = 0.3$, was reached, and then $G_{IC}$ decreased for values of $\phi_Y$ greater than 0.3 at long time. This result clearly shows that $G_{IC}$ cannot be simply related to $W_A$ as a monotonic function. We suspect that $G_{IC}$ is a function of the structure of the interfacial chains as well as $W_A$.

The relative surface energetics of the model substrates as a function of $\phi_Y$ was simply predicted using the Young−Dupré equation.

$$W_A = \gamma_1(1 + \cos\theta) \tag{8}$$

Here $\gamma_1$ and $\theta$ are the surface tension of probing liquid and the contact angle. On the basis of the water contact angle measurement, $W_A$ was determined to increase linearly from 0.064 to 0.081 J/m$^2$ as $\phi_Y$ increased from 0 to 1. These values were smaller than expected. It was believed that other hydrocarbon backbone chains or the complexity of the amine-terminated silanes on the surface are responsible for the low value of the surface energetics.[30,31] The realistic work of adhesion between −COOH and −NH$_2$ has been directly measured via interfacial force microscopy (IFM) by Thomas et al.[32] They reported that $W_A$ between well-ordered self-assembled monolayers (SAMs) with terminal −NH$_2$ groups and −COOH groups was determined to be 0.68 ± 0.062 J/m$^2$. This value of $W_A$ is about 10 times more than the $W_A$ of about 0.07 J/m$^2$ with van der Waals forces.[32,33]

**3.4. Adhesion Kinetics.** The annealing time dependence of the fracture energy of the polymer−model substrate (PBD−AlS and cPBD−AlS) interfaces is shown in Figures 8−10. No specific annealing time dependence of $G_{IC}$ is shown for the samples made from the pure PBD (Figure 8), while a strong annealing time dependence is shown for the cPBD−AlS interfaces, in the experimental time scale of 10−1000 min, depending on the surface energetics (Figure 9). The fracture energy did not change much with further annealing to 2000 min. If we compare the two characteristic cases of the $G_{IC}$ of the cPBD−AlS interface, the high energetic surface, $\phi_Y = 1$, and the low energetic surface, $\phi_Y = 0.3$, shown in Figure 10, the low energetic surface showed more than 2 orders of magnitude longer time dependence of $G_{IC}$ than the high energetic surface. This can be explained by the work done by Baumgärtner and Muthukumar.[34] They showed that the critical temperature for adsorption was lowered with the surface impurity ($CH_3$) density. Thus, it is harder for a Gaussian chain to adsorb on a chemically impure surface, $\phi_Y = 0.3$, than on a pure flat surface, $\phi_Y = 1$. In Figure 10, smaller exponents of $n = 1/4$ for $\phi_Y = 0.3$ and less than $n = 1/4$ for others are shown instead of the characteristic healing slope of $1/2$ for peel energy. Tsuji et al.[35] and Bhowmick et al.[36] observed the slope of $1/2$ for peel energy and $1/4$ for tack stress. The time dependence of the fracture energy for the Kelvin model of peel energy during the welding has a $t^{1/2}$ dependence for the elastic contribution and a $t^{1/4}$ dependence for the viscous contribution.[1] This combination of different time dependencies sometimes gives complicated time dependence of $G_{IC}$, as described by Wool[1]and Sauer et al.[28]

The adhesion strength of the polymer−solid interface develops through wetting, bond formation, and restructuring of the interface. Since PBD and cPBD were rubberlike with low glass transition temperature, full wetting contact at the interface was achieved before annealing by pressing them together. During the annealing time, the COOH groups diffuse and interact with NH$_2$ groups, forming the strong bonds through acid−base interactions, depending on the energetic driving force and the entropic constraint. Since our model surfaces have a wide range of energetic driving forces, the bonding dynamics depended on $\phi_Y$ as shown in Figures 9 and 10. The time dependence of adhesion can be compared to the reptation time of polymer chains, which was calculated by

$$T_r = \frac{R_{||}^2}{3\pi^2 D} \tag{9}$$

$$R_{||} = \left(\frac{C_\infty M j}{M_0}\right)^{1/2} b_0 \tag{10}$$

$$D \sim M^{-2} \tag{11}$$

Here $R_{||}$, $D$, $C_\infty$, $j$, $M_0$, and $b_0$ are the end-to-end distance and the self-diffusion coefficient of a polymer chain, the characteristic ratio, the number of backbone bonds per monomer, monomer molecular weight, and the bond length, respectively. Roland and Bohm[37] reported that the self-diffusion coefficient of PBD with $M_n = 84\,780$ and $M_w = 93\,258$ is $D = 3.4 \times 10^{-13}$ cm$^2$/s at 23 °C. Putting the values into the equations above gave the value of $T_r \cong 1.6$ s. The characteristic time of cPBD is expected to be the same order of the $T_r$ of PBD, which is, however, several orders of magnitude smaller than the corresponding time scale in Figures 9 and 10.

The schematic bonding dynamics of the slow and the fast adsorption cases (i.e., restructuring of a chain near an interface) is shown in Figure 11, where the unbounded chains are not shown. X represents COOH, and the gray and white sites represent NH$_2$ and CH$_3$, respectively. The higher energetic surface causes the fast segregation of COOH (case I), while the low energetic surface retards the segregation process (case II). In stage I, after the first stitching of COOH to NH$_2$, the chain dynamics changes from the snakelike reptation motion[1,2,38] of a linear chain to the star-arm-like retraction motion.[39,40] An entangled free arm adapts a new conformation above the interface by retraction along its primitive path.[42] It was known that this time scale could be very long (days), without energetic driving forces.[38,41,42] In stage 2, the unbounded COOH between

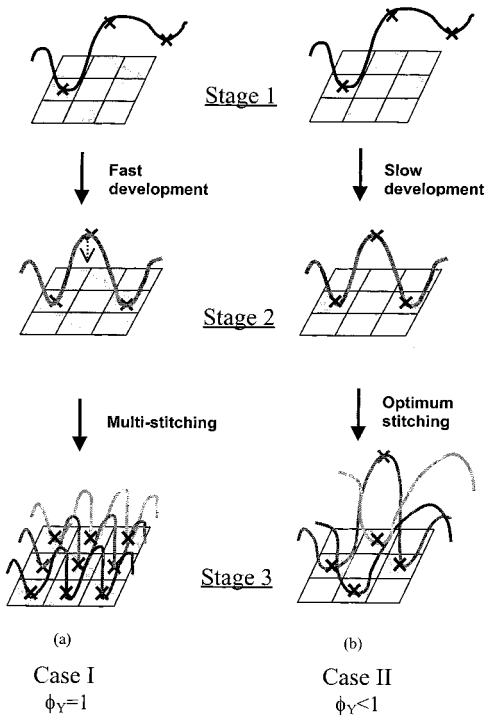


**Figure 11.** Schematic representation of interfacial chain restructuring with bond formations (a) at high energetic surface (case I; $\phi_Y = 1$) and (b) at low energetic surface (case II; $\phi_Y = 0.3$).

two anchored COOHs could only penetrate into the rest of the chains by chain excursion. Thus, a much longer restructuring time than that in the bulk is expected. The higher energetic surface (case I) may enable the chain to overcome such a hindered motion, but the reduced surface energetics (case II) limits such a motion. In stage 3, the near-equilibrium chain conformation is shown which will be described, using scaling arguments.[47] The chain confinement length, $R_\perp$, is inversely proportional to the surface energetics. In Figure 10, the restructuring time of cPBD at $\phi_Y = 0.3$ was found to be about 4 orders of magnitude and at $\phi_Y = 1$ only about 2 orders of magnitude longer than the characteristic time of polymer. However, this time dependence is much shorter than the case O'Connor and McLeish[42] described for end-grafted chains on a solid substrate approaching their equilibrium conformation with a compatible network placed on the substrate, without specific enthalphic driving forces existing between the polymer and the substrate. They expected that the adsorption strength grew on long time scales, varying exponentially with molecular weight, when entanglements dominated the motion above $T_g$.

## 4. Structure and Strength of Polymer−Solid Interface

The interface fracture energy, $G_{IC}$, measured for polymers above their glass transition temperatures can be very high due to viscoelastic losses in the polymer layer, even for bonding to rigid substrates where interdiffusion is not possible, and where no chemical or other strong bonds exist across the interface.[28] Even though the intrinsic interface strength, $G_0$, remains approximately constant,[43,44] variations of several decades in $G_{IC}$ are normally observed for polymers by changing the deformation rate, $R$, and temperature, $T$. The classic equation of interface failure is given by[44]

$$G_{IC} = G_0[1 + f(R,T)] \tag{12}$$

where $G_0$ is the intrinsic fracture energy at zero rate, and $f(R,T)$ represents the dissipation contribution from the bulk polymers where the rate and temperature dependence of the bulk viscoelastic properties are approximately interchangeable.[44,45] This equation predicts that a stronger interface (high $G_0$) allows higher stress transfer to the adhesive, causing enhanced energy dissipation in the adhesive layer. [44−46] However, if $G_0$ is too strong, the interface may not be efficient for transferring a high stress to the bulk adhesive, which is the main point of this paper. For the weak interface governed by purely dispersive (van der Waals) forces, $G_0$ is the thermodynamic work of adhesion, $W_A$[43,44] [$G_0 \cong W_A \cong 0.1$ J/m$^2$]. Andrews and Kinloch[44] effectively normalized out the huge contribution of viscoelastic dissipation in the adhesive [$1 + f(R,T)$], leaving a $G_0$ term ($W_A = 0.07$ J/m$^2$) with a model polymer on inert substrates, where only dispersive interactions exist across the interface. For the strong interfaces, dominated by chemical bonding across the interface, the values of $G_0$ at low reduced rates become much higher than $W_A$.[9] It was expected that specific bonding like hydrogen bonding or acid−base interactions in some systems would contribute to values of $G_0$ somewhat greater than $W_A$.[28]

Interface failure could be adhesive between an adsorbed chain and a substrate surface or cohesive between an adsorbed chain and other neighboring free chains, depending on the intrinsic failure energy of the interface. The failure prefers the weaker of the two that always exist at the polymer−solid interface. We suspect that the two intrinsic failure energies are not independent of each other. In this paper we experimentally showed this behavior. Now we briefly explain the relation between the two with scaling argument of an adsorbed chain. The enthalpic adsorption energy, $\Delta H$, of the chain is related to the gain of intrinsic adhesive strength $G_0^a$. Simultaneously, the entropy loss, $\Delta S$, of an adsorbed chain collapsing to the attractive surface is related to the decrease of intrinsic cohesive failure energy $G_0^c$. At equilibrium, the $\Delta S$ of an adsorbed chain can be related to the gain in $\Delta H$; thus, they are not independent of each other. We parametrized the interface structure with the entanglement sink probability (ESP) from the conformational dimension of an adsorbed chain. ESP is a function of concentration of polymer stickers, concentration of substrate receptors, and the X−Y interaction parameter. Further details of thermodynamic analysis of polymer adhesion (sticker group and receptor group effects) can be found elsewhere.[47] The brief explanation of the receptor group effect on polymer adhesion was summarized: First, a scaling concept was introduced for the conformation of an adsorbed homopolymer chain on a pure plain surface depending on the strength of X−Y interaction parameter. Then, the random copolymer was considered as a homopolymer chain by renormalizing it into blobs. Finally, for chemically rough surfaces, the pure energetic surfaces contaminated with inert impurities were modeled, and then the conformation of a chain containing blobs was considered. On the other hand, this approach was similar to that of Léger et al., who had shown similar behavior in the adhesion between the

brush and the elastomer.[48] They explained that the degree of interdigitation between them showed an optimum as a function of brush density, which governed the adhesion energy between the solid wall and an elastomer. Our trial to quantify ESP at the polymer−solid interface appeared the same with their trial to quantify the degree of interdigitation between the brush and the elastomer. We are preparing a more detailed model, using a single-chain approach (the scaling treatment of de Gennes), clearly relating the lowering of conformational entropy of the entire chain due to the attractive surface to the reduction of the entanglement sink probability (ESP) which causes the decrease of the cohesive fracture energy of the strong polymer−solid interface with increasing sticker groups or receptor groups.[47]

## 5. Conclusions

The fracture energy, $G_{IC}$, of polymer−solid interface was not a monotonic function of the surface energetics but a complicated function of an interfacial structure that appeared to be a function of sticker group concentration, receptor group concentration, and their interaction strength, as well as molecular weight, bonding time, and temperature.

The restructuring time of cPBD at the polymer−solid interface (up to 1000 min) was much longer than the characteristic time of the chain (less than 1 min). The longer restructuring time resulted from the change of the chain dynamics from the snakelike reptation motion of linear polymers to the star-arm-like retraction motion near the polymer−solid interface, which could be very long due to its exponential dependence on the molecular weight and the hindered motion near a solid wall. At long annealing time, $G_{IC}$ of the strong cPBD−AlS interface, first increased with $\phi_Y$ until the critical point, $\phi_Y^c = 0.3$, and then decreased with $\phi_Y$. The maximum $G_{IC}$ was obtained at partial coverage rather than at full coverage on the substrate. The decreasing $G_{IC}$ with further increasing $\phi_Y$ after $\phi_Y^c$ was explained: The adhesive interface strength increased between the adsorbed chains and the solid surface, while the cohesive interface strength decreased between the adsorbed chains and the other neighboring free chains with further increases in receptor density. The gain in adsorption energy was related to the increase of the adhesive interface strength, and simultaneously the entropy loss of the adsorbed chain by the strong adsorption to the attractive surfaces was related to the decrease of cohesive interface strength.

**Acknowledgment.** This work was supported by Hercules Incorporated, Wilmington, DE, and NSF-DMR-9596-267.

## References and Notes

(1) Wool, R. P. *Polymer Interface: Structure and Strength*; Hanser/Gardner: New York, 1995.
(2) de Gennes, P. G. *Soft Interface*; Cambridge University Press: Cambridge, England, 1997.
(3) Polymer/Inorganic Interface II. Presented at the MRS Symposium, 1995.
(4) Nakayama, Y.; Matsuda, T. *Macromolecules* **1996**, *29*, 8622.
(5) Ueda, T.; Matusuda, T. *Langmuir* **1995**, *11*, 4135.
(6) Uchida, E.; Uyama, Y.; Ikada, Y. *J. Polym. Sci.* **1989**, *27*, 527.
(7) Mittal, K. L. *Polymer Surface Modification: Relevance to Adhesion*; Uthrecht, The Netherlands, 1996.
(8) Stralin, A.; Hjertberg, T. *Surf. Interface Anal.* **1993**, *20*, 337.
(9) Mclaren, A. D.; Seiler, C. J. *J. Polym. Sci.* **1949**, *4*, 63.
(10) Mao, T. J.; Reegen, S. L. In *Adhesion & Cohesion*; Weiss, P., Ed.; Elsevier Publishing Company: Amsterdam, 1962; p 109.
(11) Schultz, J.; Lavielle, L.; Carre, A.; Comien, P. *J. Mater. Sci.* **1989**, *24*, 4363.
(12) Gong, L.; Friend, A. D.; Wool, R. P. *Macromolecules* **1998**, *31*, 3706.
(13) Gutman, L.; Chakraborty, A. K. *J. Chem. Phys.* **1994**, *101*, 10074.
(14) Beck Tan, N. C.; Peiffer, D. G.; Briber, R. M. *Macromolecules* **1996**, *29*, 4969.
(15) Fowkes, F. M.; Mostafa, M. A. *Ind. Eng. Chem. Prod. Res. Dev.* **1978**, *17*, 3.
(16) Donnet, J. B. *Pure Appl. Chem.* **1981**, *53*, 2223.
(17) Harding, P. H.; Berg, J. C. *J. Adhes. Sci. Technol.* **1997**, *11*, 471.
(18) Gong, L.; Wool, R. P.; Friend, A. D.; Konstantin, G. J. *J. Polym Sci., Polym. Chem.* **1999**, *37*, 3129.
(19) Arkles, B. *Chemtech* **1977**, *7*, 766.
(20) Plueddemann, E. *Silane Coupling Agents*; Plenum: New York, 1982.
(21) Lenk, T. J.; Hallmark, V. M.; Rabolt, J. F.; Haussling, L.; Ringsdorf, H. *Macromolecules* **1993**, *26*, 1230.
(22) Offord, D. A.; Griffin, J. H. *Langmuir* **1993**, *9*, 3015.
(23) Lee, I.; Wool, R. P. Manuscript in preparation.
(24) Folkers, J. P.; Laibinis, P. E.; Whitesides, G. M. *Langmuir* **1992**, *8*, 1330.
(25) Harding, P. H.; Berg, J. C. *J. Appl. Polym. Sci.* **1988**, *67*, 1025.
(26) Offord, D. A.; Griffin, J. H. *Langmuir* **1993**, *9*, 3015.
(27) Ahagon, A.; Gent, A. N. *J. Polym. Sci., Polym. Phys. Ed.* **1975**, *13*, 1285.
(28) Sauer, B. B.; Gochanour, C. R.; Van Alsten, J. G. *Macromolecules* **1999**, *32*, 2739.
(29) De Gennes, P.-G. *C. R. Acad. Sci., Ser. 2* **1991**, *312*, 1415.
(30) Chu, C. W.; Kirby, D. P.; Murphy, P. D. *J. Adhes. Sci. Technol.* **1993**, *7*, 417.
(31) Urban, M. W. *J. Adhes. Sci. Technol.* **1993**, *7*, 1.
(32) Thomas, R. C.; Houston, J. E.; Crooks, R. M.; Kim T.; Michalske, T. A. *J. Am. Chem. Soc.* **1995**, *117*, 3830.
(33) Andrew, E. H.; Kinloch, A. J. *Proc. R. Soc. London* **1973**, *332*, 385.
(34) Baumgärtner, M.; Muthukumar, M. *J. Chem. Phys.* **1991**, *94*, 4062.
(35) Tsuji, T.; Masuoko, M.; Nakao, K. In *Adhesion and Adsorption of Polymers*; Lee, L. H., Ed.; Plenum Press: New York, 1980; *Polym. Sci. Technol.* **1980**, *12A*, 439.
(36) Bhowmick, A. K.; De, P. P.; Bhattacharyya, A. K. *Polym. Eng. Sci.* **1987**, *27*, 1195.
(37) Roland, C. M.; Bohm, G. G. A. *Macromolecules* **1985**, *18*, 1310.
(38) Doi, M.; Edwards, S. F. *The Theory of Polymer Dynamics*, Clarendon Press: Oxford, 1986.
(39) Ajdari, A.; Rubinstein, M.; Leibler, L.; Brochard-Wyart, F.; de Gennes, P. G. *C. R. Acad. Sci. Paris III* **1993**, *316*, 317.
(40) Field, J. B.; Toprakioglu, C.; Dai, L.; Hadziioannou, G.; Smith, G.; Hamilton, W. *J. Phys. II* **1992**, *2*, 2221.
(41) Ferry, J. D. *Viscoelastic Properties of Polymers*, 3rd ed.; John Wiley & Sons: New York, 1980.
(42) O'Connor, K.; McLeish, T. *Faraday Discuss.* **1994**, *98*, 67.
(43) Gent, A. N.; Hamed, G. R. *Proc. R. Soc. London, A* **1969**, *310*, 433.
(44) Andrews, E. H.; Kinloch, A. J. *Proc. R. Soc. London, A* **1973**, *332*, 385.
(45) Gent, A. N.; Hamed, G. R. *Plast. Rubber Proc.* **1978**, *3*, 17.
(46) Brown, H. R. *Annu. Rev. Mater. Sci.* **1991**, *21*, 463.
(47) Lee, I.; Wool, R. P. Manuscript in preparation.
(48) Léger, L.; Raphäel, E.; Hervet, H. *Adv. Polym. Sci.* **1999**, *138*, 185.

MA991037A